EXAFS: NEW TOOL FOR STUDY OF BATTERY AND FUEL CELL MATERIALS

James McBreen and William E. O'Grady
Brookhaven National Laboratory
Upton, New York 11973

Kaumudi I. Pandya
Case Western Reserve University
Cleveland, Ohio 44106

Extended X-ray absorption fine structure (EXAFS) is a powerful technique for probing the local atomic structure of battery and fuel cell materials. The major advantages of EXAFS are that both the probe and the signal are X-rays and the technique is element selective and applicable to all states of matter. This permits in situ studies of electrodes and determination of the structure of single components in composite electrodes, or even complete cells. EXAFS specifically probes short range order and yields coordination numbers, bond distances, and chemical identity of nearest neighbors. Thus, it is ideal for structural studies of ions in solution and the poorly crystallized materials that are often the active materials or catalysts in batteries and fuel cells. This paper uses studies on typical battery and fuel cell components to describe the technique and the capability of EXAFS as a structural tool in these applications. Typical experimental and data analysis procedures are outlined. The advantages and limitations of the technique are discussed. Other techniques, using high intensity synchrotron X-rays are also briefly discussed.

INTRODUCTION

The performance and life of batteries and fuel cells are often determined by subtle aspects of the structure of various components. Examples of these interrelationships are as follows: 1) Lead-acid battery life is determined by the structure of the basic lead sulfates in the cured plates (ref. 1). 2) Zinc-manganese dioxide battery performance strongly depends on the structure of MnO_2 (ref. 2). 3) Swelling of nickel electrodes is related to the structure of $Ni(OH)_2$ (ref. 3). 4) The activity and stability of carbon supported platinum catalysts are dependent on strong carbon platinum interactions (ref. 4). 5) The quality of zinc deposits in flow batteries (ref. 5) and the efficiency of redox systems are related to electrolyte structure (ref. 6-7).

Structural determinations of battery and fuel cell electrode materials are often very difficult. The situation is exacerbated when in situ determinations are attempted. Often these materials are amorphous and exhibit very weak or even no X-ray diffraction patterns. Examples are $Ni(OH)_2$, NiOOH (ref. 8), MnO_2 (ref. 9), and pyrolyzed metal-macrocyclic electrocatalysts (ref. 10). Many battery materials such as NiOOH and the discharge products of MnO_2 are hydrated so meaningful ex situ measurements using various photoelectron spectroscopies are nearly impossible. Some in situ methods are of limited value because they require specular surfaces (reflectance spectroscopy and ellipsometry) or are applicable only to a few elements

(Mossbauer spectroscopy and SERS (surface enhanced Raman spectroscopy)). Interpretation of spectroscopic data (e.g. Raman spectroscopy or photoacoustic spectroscopy (PAS)) from a typical electrode containing additives, conductive diluents, electrolyte and plastic binders is essentially impossible.

Determination of the structure of electrolytes is also a problem. The application of various scattering (e.g. Raman) and absorption (e.g. infrared and nuclear magnetic resonance (NMR)) spectroscopies to electrolyte studies has been critically reviewed (ref. 11). In many cases the lack of a reliable theoretical framework has led to conclusions that are qualitative in character. This is particularly true when the spectroscopies are applied to hydrated ions. For instance the Raman method is not able to yield information about ion-water distances in solution. In the case of neutron scattering, even in concentrated solutions, ion-water contributions to the total scattering pattern are only ~10%. This makes elucidation of the ion-water terms very difficult.

The present paper discusses how EXAFS can help in these structural determinations. The basic principles, the experimental methods, and data analysis for EXAFS will be outlined. This will be done using examples of EXAFS studies on typical battery and fuel cell components.

THE EXAFS TECHNIQUE

Experimental Aspects: An EXAFS experiment is simply the accurate determination of the X-ray absorption coefficient (μ) of a material, as a function of photon energy, in an energy range that is below and above an absorption edge of one of the elements in the material. The most direct method is to do a transmission X-ray absorption experiment. Figure 1 is a schematic representation of the experimental configuration. It consists of an X-ray source, a double-crystal monochromator, a thin sample of the material, detectors for monitoring the X-ray beam before and after it passes through the material, and a data acquisition system. The data acquisition system is used for several purposes. This includes stepping the monochromator to pass the desired photon energies (E), alignment of the sample in the beam and monitoring the signals from the detectors.

The Origin of EXAFS: EXAFS is the result of a photoelectric absorption process. In most cases X-ray absorption involves the interaction of X-rays with the outer shell electrons of elements. This can be described by the simple Lambert equation

$$I = I_o \exp(-\mu x) \qquad (1)$$

where I_o is the intensity of the incident photon beam, I the intensity of the transmitted beam, and x the thickness of the sample. Figure 2 is a X-ray absorption spectrum for a dry plastic bonded nickel oxide electrode. The initial monotonically decreasing part of the curve, where μ is approximately proportional to E^{-3}, can be described by equation (1) and is determined by the chemical composition of the electrode including all the elements in the conductive diluent, the $Co(OH)_2$ additive and the plastic binder. When the X-ray energy (8337 eV) is sufficient to liberate an inner nickel K-shell electron, and excite it to an unoccupied continuum state, an abrupt increase in the absorption is observed. This is called the absorption edge and is unique to the element. For photon energies greater than E_b = 8337 eV, the ejected photoelectron travels as an outgoing spherical wave with a wavelength (λ)

$$\lambda = \frac{2\pi}{k} \tag{2}$$

where k, the photoelectron wave vector

$$k = \left\{\frac{2m}{\hbar^2}\ (E-E_b)\right\}^{1/2} \tag{3}$$

where $E = \hbar\omega$ is the energy of the incident photons, m is the electron mass, and h is Planck's constant divided by 2. If the nickel atoms had no neighbors (e.g. as in an inert gas) then μ would continue to decrease with a smooth $\sim E^{-3}$ dependence beyond the absorption edge. However, neighbor oxygen and nickel atoms in the β-$Ni(OH)_2$, backscatter a small fraction of the outgoing photoelectron wave. Interference between the outgoing wave and the incoming waves from neighboring atoms, modulates the photoelectron wave function in the nickel core region, and results in the sinusoidal variation of μ versus E. This yields the EXAFS (χ) - the oscillations in the absorption that extend for about 1000 eV above the absorption edge. In energy space, the EXAFS - $\chi(E)$ is defined as

$$\chi(E) = \frac{\mu(E) - \mu_o(E)}{\mu_o(E)} \tag{4}$$

where $\mu(E)$ is X-ray absorption coefficient and $\mu_o(E)$ a hypothetical absorption coefficient of the nickel with no surrounding atoms. The $\chi(E)$ function can be converted to photoelectron wave vector (k) space by the relationship in equation (2). The physical basis for $\chi(k)$ has been worked out (ref. 12) and is given in its simplest form by

$$\chi(k) = \sum_j \frac{N_j}{R_j^2}\ B_j(k)\ \exp(-2k^2\sigma^2_j)\ \exp(-R_j/\lambda(k))\ \mathrm{Sin}[2kR_j+\phi_j(k)] \tag{5}$$

where N_j refers to the coordination number in a shell of identical atoms, R_j is the respective coordination distance, F_j is the backscattering amplitude of the coordinating atoms, σ_j is the root mean square variation in R_j due to static or thermal disorder (the Debye-Waller factor), $\lambda(k)$ is the mean free path of the photoelectron, and $\phi_j(k)$ is a phase shift due to the photoelectron traversing the distance R_j twice and encountering the potential of the scatter atom once, and that of the absorbing atom twice. The EXAFS is a summation of the effects of different shells of atoms. For a simple case such as a hydrated ion with one coordination shell, the EXAFS is a simple sinusoidal function whose frequency depends on R and the amplitude on the hydration number N. Figure 3 shows the EXAFS for β-$Ni(OH)_2$. It consists of the summation of at least three sinusoidal waves.

This is a rather simplified description of EXAFS. More details are provided in several excellent reviews (ref. 13-15). From this description it is evident that the EXAFS contains a lot of information about the coordination of the excited atom.

Preliminary Data Analysis - The First Fourier Transformation: The aim of data analysis is the determination of the unknown quantities in equation (5). The quantities of most interest to chemists are R_j, N_j, and σ_j. The first step is a Fourier transformation of $\chi(k)$. Equation (5) is the superposition of an unknown

number of coordination shells. Fourier transformation of $\chi(k)$ yields peaks in r space corresponding to individual shells around the absorbing atom. The Fourier transform is given by

$$\theta_n(r) = \frac{1}{(2\pi)^{1/2}} \int_{kmin}^{kmax} k^n \chi(k) \exp(2ikr)\, dk \qquad (6)$$

The function $\theta_n(r)$ is called a radial structure function and it contains a series of peaks whose positions R_j are related to the coordination distances. Figure 4 is a Fourier transform of the data in figure 3. The first peak corresponds to the Ni-O coordination and the second peak to the first Ni-Ni shell in the brucite structure plane. These peaks are shifted to R values that are lower than the actual Ni-O and Ni-Ni distances because of the phase shift $\phi_j(k)$.

Reduction of the raw data in figure 2 to the radial structure function in figure 4 requires several mathematical manipulations. This includes subtraction of the background, normalization of the EXAFS oscillations and the Fourier transformation. Background subtraction includes a fitting of the pre-edge portion in the spectrum in figure 2, to within 50-70 eV of the edge and extrapolation to the energy region where the EXAFS is present. In this way, the contributions of atoms other than nickel are determined. Fitting is terminated below the edge because of pre-edge features that occur, particularly with transition metals. The EXAFS data are removed from the measured data by subtraction of a cubic spline background. A powerful method for checking whether this is done properly is to examine the derivative of the background and by an iterative technique and a smoothing parameter continue the process until the residual EXAFS oscillations are barely visible in the background derivative. The next step is to normalize the EXAFS by dividing by the height of the absorption edge ($\Delta\mu$) which is usually taken at 50 eV above the absorption edge. To reduce termination errors in the Fourier transform the values of k_{min} and k_{max} are chosen to coincide with nodes in the $\chi(k)$ function. It is a relatively simple process to reach this first stage in the data reduction. Often this suffices, particularly if one wants to only "fingerprint" a material in the same way as diffraction patterns are used. An example is given in figure 5 where radial structure functions for cobalt metal foil and pyrolyzed cobalt phthalocyanine on Vulcan XC-72 carbon are shown. The pyrolysis product at 900°C in argon is obviously cobalt.

Final Data Analysis - Determination of R_j, N_j, and σ_j: After the first Fourier transform is obtained the next step is isolation of the contributions of each shell. In cases like β-$Ni(OH)_2$, where the peaks of the Fourier transform do not overlap (figure 4), the contribution from each shell can be isolated by doing an inverse transform of single peaks back to k-space. All other peaks, except the one of interest, are set to zero. Thus, the individual χ_j is isolated. Figure 6 shows an inverse transform of the first peak in figure 4. The result is a simple sinusoidal wave of a single shell scatterer.

Once χ_j is isolated, the next step is a separate analysis of the phase ($\Phi(k)$) and amplitude ($A(k)$) functions in equation (5). These are respectively

$$\Phi(k) = 2kR + \phi(k) \tag{7}$$

and

$$A(k) = \frac{N}{R^2} \; B(k) \; \exp(-2k^2\sigma^2) \; \exp(-R/\lambda(k)) \tag{8}$$

Determination of N, R,and σ depends on knowing B(k), $\phi(k)$ and $\lambda(k)$. The best way of doing this is by comparison with standard compound(s) of known structure, having identical absorbers and backscatters to the unknown (u). In this case the standard compound NiO, which has a rock salt structure and a Ni-O distance of (R_s = 2.08Å), and a coordination number of (N_s = 6). The Debye-Waller factor is given a value σ_s = 0. So the disorder of β-$Ni(OH)_2$ is determined relative to NiO. The quantities of B(k), $\phi(k)$ and $\lambda(k)$ are assumed to be "transferable" from the standard to the unknown. For NiO $\phi_u(k_u)$ can be calculated. Then for β-$Ni(OH)_2$ which is the unknown

$$\phi_u(k_u) = \phi_s(k_s)$$

After minor corrections for the inner potential (ΔE_o) - differences in absorption edge position for β-$Ni(OH)_2$ and NiO - R_u is calculated as 2.067Å from

$$R_u = [\Phi(k) - \phi_s(k_s)]/2k$$

This is the N-O distance in β-$Ni(OH)_2$. Thus, phase analysis yields actual bond lengths which are somewhat higher than R_j in the radial structure function (figure 4).

The value of R_u is then used to do an amplitude analyses for the determination of N_u and σ_u. Since σ_u is in a k-dependent term it can be separated from N_u by a simple ratio method involving the logarithms of the ratio of the single shell amplitudes of the unknown and the standard

$$\ln \frac{A_u(k)}{A_s(k)} = \ln \frac{N_u R_s^2}{N_s R_u^2} - \frac{2(R_u - R_s)}{\lambda(k)} - 2k^2(\sigma_u^2 - \sigma_s^2)$$

The k dependence of λ can be neglected so a plot of $\ln[A_u(k)/A_s(k)]$ vs k^2 yields a straight line of intercept

$$\ln \frac{N_u R_s^2}{N_s R_u^2}$$

and slope

$$2(\sigma_u^2 - \sigma_s^2) = 2\Delta\sigma^2$$

Thus, N_u, R_u, and $\Delta\sigma^2$ can be determined. The term $\Delta\sigma^2$ gives the relative disorder for Ni-O in β-$Ni(OH)_2$. The respective values for N_u, R_u, and $\Delta\sigma^2$ are 5.96, 2.067Å and -0.00124. Data analysis can be done using theoretical values of the phase and amplitude functions (ref. 16).

This data analysis is relatively simple, since the first two shells are well separated and are of widely different atomic numbers (Z). The situation is much more complicated when there are overlapping shells of similar Z value. Examples of these are reported in the literature (ref. 17). A recent book (ref. 18) gives further details of data analysis.

X-ray Sources for EXAFS Studies: The choice of source of X-rays for EXAFS studies are the bremsstrahlung from a rotating anode X-ray tube or synchrotron radiation from electron or positron storage rings. The EXAFS (fig. 2) are only about 5% of total absorption. Signal-to-noise ratios (S/N) of greater than 100 are required to determine the EXAFS accurately. Since S/N is proportional to the square root of the X-ray intensity, a high flux of X-ray photons is required. The intensity of a synchrotron source is about 10^4-10^6 times higher than from a conventional X-ray tube. This reduces measurement time for a typical EXAFS experiment from a week or more to less than half an hour. Synchrotron radiation also permits studies of dilute samples, including additives and the metallic constituents of metal macrocyclics. Figure 7 shows the EXAFS spectra for the cobalt additive in the nickel oxide electrode of figure 2. Even though the additive is dilute, the spectrum is excellent. However, conventional sources are sometimes convenient. A unit with a rotating anode for electrolyte studies has been recently described (ref. 19).

Near Edge Structure - XANES: The X-ray absorption near edge structure (XANES) portion of the spectrum - within 30 eV of the edge - contains chemical information about the absorbing atom. It depends on the oxidation state of the excited atom, the coordination geometry and the type of ligands. There is an excellent review of early work in this area (ref. 20). The absorption edge energy shifts linearly with valence state and follows Kunzl's law (ref. 21). XANES is an area of very active experimental and theoretical work. Further theoretical developments will permit its use for a variety of coordination chemistry studies.

Dispersive EXAFS: At present there are two facilities, one in France (ref. 22), and the other in Japan (ref. 23), for time resolved EXAFS studies. The technique uses a bent triangular crystal to focus and disperse the quasi-parallel polychromatic X-ray beam from a synchrotron. The sample of interest is placed in the focal point of the beam. The transmitted beam then diverges towards a position sensitive detector. The one in France consists of 1024 sensing elements (2500 μ high x 25μ wide). This permits acquisition of high quality XANES and EXAFS spectra in times as short as 16 msec. With the advent of detectors with faster response, even shorter times can be achieved. The technique permits in situ time resolved kinetic studies.

APPLICATIONS OF EXAFS AND DESIGN OF EXPERIMENTS

EXAFS is the preferred technique for in situ structural studies in electrochemical cells, since both the probe and the signal are X-rays. It is often the only suitable technique for amorphous materials or components of composite structures. It is useful for the study of any element with an atomic number of 16 and above. Once EXAFS is chosen, the important experimental design aspects are sample preparation, the choice of suitable standards and the method for detection.

The simplest method of detection is to do transmission EXAFS using the setup shown in figure 1. For these experiments, uniformity of the sample is important. If possible, the sample should be chosen to give an absorption of $\Delta\mu x \sim 1.5$ at the edge of interest. Several methods for preparation of uniform solid samples are described in the literature (ref. 24-26). Most methods used by battery and fuel cell technologists for preparing of electrodes and separators are useful for preparing samples. One method that the authors have used is a vacuum table technique for casting samples (ref. 27, 28). It is important that the samples be pinhole free and free from cracks. If the elemental composition of a sample is known, the mass of material (M) needed to form a specimen with the desired absorption characteristics can be calculated from the equation

$$M = \frac{A \ \ell n(I_o/I)}{\sum_j f_i(\mu/\rho)_i} \qquad (12)$$

where A is the sample area, f_i is the weight fraction of the ith element in the sample, and $(\mu/\rho)_i$ is the mass absorption coefficient of the ith element at the wavelength of interest. Compilations of $(\mu/\rho)_i$ may be found in a report by McMaster (ref. 29). Summary tables are also given in the most recent editions of the CRC Handbook of Chemistry and Physics (ref. 30). A value of $\ell n(I_o/I) = \Delta\mu x \sim 1.5$ usually gives the best results. However, if a sample contains two or more stong absorbers (e.g. $ZnBr_2$) or is inherently very dilute (e.g. carbon supported platinum catalysts) then lower values of $\Delta\mu x$ may have to be used. However, good data can be obtained with $\Delta\mu x$ values as low as 0.05.

In situ transmission EXAFS of carbon supported platinum electrodes has been done in operating phosphoric acid fuel cells (ref. 31), using a slightly modified version of a cell that was previously described (ref. 32). A cell was designed for in situ studies of the charge/discharge processes of plastic bonded nickel oxide electrodes (ref. 28). This is shown in figure 7. Equation (12) can be used in the design of cells of this type. Absorbence of cell components in the X-ray path have to be taken into account. It is important that no inhomogeneity such as current collector wires be in the path of the beam. Carbon current collectors such as Grafoil are best. Bubbles in electrolyte samples and cells should also be avoided.

For liquid samples such as electrolytes, a sample chamber like that shown in figure 9 is suitable. The chamber thickness can be varied depending on electrolyte concentration. The thickness can be calculated using equation (12).

It is important to use good standards which have known excited atom/backscatter coordination. The Fourier transforms for these should have single well separated peaks. Thus, ferrocene is a good Fe-C standard, whereas cobaltocene is not a good Co-C standard. The latter has two Co-C distances and overlapping peaks in the Fourier transform. Metal foil stndards are usually good for M-M standards, except for b.c.c. metals where the first and second shells overlap.

Apart from transmission measurements, other detection schemes are fluorescence measurements and electron detection. These methods are reviewed in the literature (ref. 14, 33). Fluorescence methods are very good for working with dilute samples - down to about 100 ppm. Electron detection schemes are useful for investigating processes occurring within a few hundred Angstroms of a surface. With the fluorescence method, homogeneity of the sample is not as critical as in transmission measurements. With electron detection a smooth sample surface appears to be important.

Several synchrotron sources are now available for EXAFS measurements, their locations and characteristics are given in two recent reviews (ref. 34-35). Several other souces are under construction or are planned (ref. 36). Since the time available at these sources is usually limited, it is very important, particularly in the case of in situ measurements, to have electrodes and cells that are functioning properly before doing the EXAFS measurements.

EXAFS STUDIES OF BATTERY AND FUEL CELL MATERIALS

Even though extensive application of the EXAFS technique is recent, there have been several publications on materials related to batteries and fuel cells. These are briefly reviewed.

Aqueous Electrolytes: Early work on the application of EXAFS to aqueous electrolyte studies has been reviewed (ref. 13). The EXAFS technique is unique in that it can sort out ion-ion and ion-water interactions unambiguously. Lagarde et al. (ref. 37) used EXAFS in a study of $ZnBr_2$ solutions in the concentration range 0.089 - 8.08 M. In going from the lower to the higher concentrations the bromide coordination number increased from 1 to 3.5 and waters of hydration decreased from 7 to 2.5. The Zn-Br bond length was 2.37Å and the Zn-O bond length was 1.94Å. Aliotta et al. (ref. 38) did an EXAFS study of mixed $ZnBr_2$-$CuBr_2$ and mixed $ZnBr_2$-$SrBr_2$ solutions. In both cases it was found that the $CuBr_2$ and $SrBr_2$ acted as bromine donors and that the mean coordination value for bromide ions around zinc increased to four as the bromide to zinc ion ratio increased. Similar increases in the coordination value for bromide ions have been observed on addition of either HBr or $AlBr_3$ to $ZnBr_2$ electrolytes (ref. 39). Other studies of interest to battery researchers are EXAFS investigations of Ni^{2+} ions in concentrated $Ni(NO_3)_2$ solutions (ref. 40), Mn^{2+} ions in $MnCl_2$ solutions (ref. 41), and the Jahn-Teller complexes of $Cu(H_2O)_6^{2+}$ and $Cr(H_2O)_6^{2+}$ (ref. 42).

Polymeric Electrolytes: EXAFS of iron, in iron neutralized Nafion ionomers, has been used to probe ion aggregation in the membrane (ref. 43). This has been done in hydrated and dried membranes.

The poly ethylene oxide (PEO) complexes - $RbSCN(PEO)_4$, $RbSCN(PEO)_4$ and $RbI(PEO)_8$ - have been investigated using EXAFS (ref. 44). These materials are amorphous at room temperature. The results showed that Rb is in well defined sites of four coordination with ether oxygens, with the actual configuraton being anion dependent. In the case of iodide, there are two long and two short Rb-O bonds with the iodide outside the first coordination shell at 3.7Å. The thiocyanate complexes have a single set of oxygen neighbors and the N atom of the thiocyanate group appears to be also located within the first shell.

Linford et. al. (ref. 45) have done Cu EXAFS on electrolyte from the system

$$M\,|\,CuI + \text{sulfonium iodide}\,|\,I_2 - \text{perylene}$$

Measurements were made on a fresly prepared electrolyte (a 5.5:1 CuI-4 methyl-1,4-oxathianium iodide adduct) and an electrolyte from a cell after 2000 h of discharge. These results show that the starting electrolyte consists mainly of γ-CuI. After discharge sulfur appears to be incorporated in the first coordination shell of copper, implying decomposition of the sulfonium cation.

Solid Oxide Electrolytes: There has been one EXAFS study of yttria-stabilized zirconia over the temperature range -120° to 770°C (ref. 46). Both Y and Zr EXAFS were obtained in 18 wt % Y_2O_3-stabilized zirconia. The results indicate that at low temperatures the anion vacancies are preferentially sited closer to the Zr^{4+} ions. This displaces the Zr^{4+} ions from their centrosymmetric sites. Increasing the temperature leads to a random distribution of anion vacancies. Recent results on calcia-stabilized zirconia (ref. 47) indicate that the vacancies are also associated with the Zr^{+4} ions. Similar effects have been observed for 40% Y_2O_3 in Bi_2O_3 (ref. 48).

In Situ Studies in Cells: In situ EXAFS has been done on the ferrocyanide/ferricyanide system in a thin layer spectroelectrochemical cell (ref. 49). The results show that the Fe-C bond length is 0.03Å shorter in the ferricyanide than in the ferrocyanide complex.

In situ EXAFS studies have also been done on plastic bonded nickel oxide electrodes (ref. 26, 50). During oxidation of $Ni(OH)_2$ to NiOOH there is a contraction along the a axis of the $Ni(OH)_2$ brucite structure. The Ni-O distance decreases from 2.04Å to 1.88Å. The first Ni-Ni distance also decreases from 3.16°Å to 2.87Å. On discharge the interatomic distances revert to the original values. During the formation cycles considerable disorder is generated in the $Ni(OH)_2$ structure.

Electrocatalysts: Extensive work has been done using EXAFS to study metal catalysts on non-conductive supports. This work has been reviewed (ref. 51). A good example of the capabilities of the technique are the papers of Koningsberger and his co-workers (ref. 17, 52-54), which includes work on platinum supported on alumina. Other platinum catalysts, including the Adams catalyst have been investigated (ref. 55). The results indicate that it is a disordered form of α-PtO_2. Recently, EXAFS has been used to study metal-carbon interactions in carbon supported platinum catalysts in fuel cell electrodes (ref. 56). The data indicate two types of Pt-C interactions.

There is one report on EXAFS studies of pyrolysed cobalt porphyrin catalyst supported on active carbon (ref. 57). The results have been interpreted on the basis that a CoN_4 group is retained in the heat treated catalyst.

Battery Materials: EXAFS has been used to study several battery materials such as metal chalcogenides (ref. 58) and superionic conductors (ref. 59). Work on other materials of interest to battery research are to be found in several reviews (ref. 13-15, 34, 60, 61).

XANES STUDIES OF BATTERY AND FUEL CELL MATERIALS

XANES has been used recently to investigate several battery and fuel cell related materials. These include an investigation of the cerous/ceric redox system (ref. 62), the interaction of carbon monoxide with ferric tetrasulfophthalocyanine in alkaline solution (ref. 63), a study of vanadium oxides in various oxidation states (ref. 64) and an investigation of high temperature corrosion of Fe-Cr alloys (ref. 65).

In a recent study (ref. 66), XANES spectra were used to detect a SiO_2 like layer at the interface between nickel and a yttria-stabilized zirconia electrolyte. Linford et. al. (ref. 45) also used XANES to identify changes in the copper environment after discharging cells.

An interesting application of XANES is its use as a quantitative technique for the determination of the number of unoccupied d-electron states in platinum catalysts (ref. 67).

SYNCHROTRON RADIATION AND FUNDAMENTAL ELECTROCHEMICAL STUDIES

The application of synchrotron radiation to fundamental studies of the electrode/electrolyte interface has really only begun. Recent results on the adsorption of iodine on platinum (111) show that the technique can be applied to monolayers (ref. 68). It has also been shown that various fluorescence and electron detection schemes can be used (ref. 69). Electron-yield EXAFS data have been successfully obtained from a nickel surface covered with a thin film of water (ref. 70). Recently the X-ray standing wave technique has been used to study iodine and copper layers on platinum (ref. 71). Several other synchrotron radiation techniques have been used for the study of chemisorbed atoms and molecules. These have been reviewed (ref. 72) and some are applicable to electrochemical systems. Another promising technique for fundamental studies is X-ray topography (ref. 73). Many of these techniques, such as X-ray standing wave and X-ray topography, are old but synchrotron radiation greatly reduces data acquisition times.

ADVANTAGES OF EXAFS AND FUTURE APPLICATIONS

Progress in basic and applied electrochemical research has been hampered because of the lack of a technique for *in situ* studies at a molecular level (ref. 74). The small amount of work so far indicates that synchrotron radiation techniques will change this. The EXAFS technique is versatile in that it is element specific and can be applied to most elements in the periodic table. Furthermore, it can be applied to all states of matter, whether they be solids, liquids, gases, or absorbed monolayers. It is an excellent technique for investigations of dilute systems. Together with XANES it yields both chemical and structural information.

Unlike X-ray diffraction of single crystals, EXAFS is not an *ab initio* structural determination technique. However, many battery active materials, electrolytes and electrocatalysts cannot be prepared as single crystals. EXAFS is the best technique for studying these amorphous materials. With a careful choice of standards and exhaustive data analysis for phase and amplitude, unknown coordinating atoms can be determined by EXAFS. The relative merits of EXAFS and diffraction have been recently reviewed (ref. 75).

From a basic point of view, the greatest impact of these X-ray techniques will be new insights into the electrode/electrolyte interface. It will also attract scientists from other disciplines to electrochemistry. In practical applications, it will permit *in situ* studies of active material and catalyst preparation,

including catalyst-support interactions. The investigation of performance limiting and degradation mechanisms can be studied in actual cells at a molecular level. EXAFS is an excellent technique for investigating disordered materials and materials with defects. An example of the latter are transformation toughened ceramics. With the advent of more synchrotron sources (ref. 34-36) and the development of more simplified data analysis packages the technique will find widespread use.

ACKNOWLEDGMENTS

The data reported in the figures in this paper were obtained at Beam Line X-11 of the National Synchrotron Light Source at Brookhaven National Laboratory. The authors thank the Department of Energy, Division of Materials Sciences for operating funds for Beam Line X-11, under Contract DE-AC05-80ER10742.

LIST OF SYMBOLS

A	Sample area
$A(k)$	Amplitude of EXAFS as a function of k
$A_s(k)$	Amplitude of EXAFS for standard excited atom - backscatterer combination
$A_u(k)$	Amplitude of EXAFS for unknown compound
$A_j(k)$	Amplitude of EXAFS for a particular coordination shell j of the same type of atoms at a distance R_j from the excited atom
$B(k)$	The backscattering amplitude of neighbor atoms around the excited atom; the substripts s, u and j have the same meaning as for A(k)
E	Energy of the X-ray photon
E_b	Binding energy of a core electron in the absorber atom
f_i	Weight fraction of an element i in a sample
I	Intensity of transmitted X-ray beam
I_o	Intensity of incident X-ray beam
k	Wave vector of ejected photoelectron
m	Mass of the electron
N_j	Coordination number for a single shell j of backscatterers; the subscripts s and u have the same meaning as for A(k)
R_j	The distance between an absorber atom and a single shell j of backscatterers; the subscripts s and u have the same meaning as for A(k)

x	Sample thickness
$\hbar$	Plancks constant divided by 2
$\theta_n(r)$	Fourier transfer of the EXAFS, called the radial structure function
λ	Wavelength of the photoelectron
$\lambda(k)$	Mean free path length of the photoelectron
μ	X-ray absorption coefficient of a sample
$\mu(E)$	X-ray absorption coefficient of an absorber as a function of photon energy
$\mu_o(E)$	X-ray absorption coefficient of an absorber without any backscatterers
$(\mu/\rho)_i$	Mass absorption coefficient of the element i
σ_j	Deviation in R_j caused by static and thermal disorder of the backscatterer j
$\Delta\sigma_j^2$	Debye-Waller factor - deviation of σ^2 with respect to some standard
$\phi_j(k)$	The phase shift due to a single shell of backscatterers j; the subscripts s and u have the same meaning as for A(k)
Φ	The argument of the Sin term in the EXAFS - equation 5
χ	The EXAFS
ω	Radial frequency of X-ray photon

REFERENCES

1. Biagetti, R. V. and Weeks, M. C. Bell. Syst. Tech. J., 49 (1970) 1305.

2. Brodd, R. J., Kozawa, A. and Kordesch, K. V., J. Electrochem. Soc., 125., (1978) 271c.

3. Pickett, D. F., Martin, U. D., Logsdon, J. W. and Leonard, J. F., Proc. 27th Power Sources Symp., PSC Publications, Red Bank, NJ (1976), pp. 120-3.

4. Ehrburger, P., Mahajan, D. P. and Walker, Jr., P. L., J. Catalysis, 43 (1976) 61.

5. McBreen, J. and Gannon, E., J. Electrochem. Soc., 130 (1983) 1667.

6. Gahn, R. F., Hagedorn, N. H. and Ling, J. S., Proc. Intersoc. Energy Convers. Eng. Conf., 18th (Vol. 4) (1983) 1647-52, CA, 99:161425b.

7. Peter, L. M., Durr, W., Bindra, P. and Gerischer, H., J. Electroanal. Chem., 71 (1976) 31.

8. Barnard, R., Randell, C. F. and Tye, F. L., J. Applied Electrochem., 10 (1980) 109.

9. Brenet, J. P. and Ghosh, S., Electrochim. Acta, 7 (1962) 449.

10. Wiesener, K., Electrochim. Acta, 31 (1986) 1073.

11. Enderby, J. E. and Neilson, G. W., Rep. Prog. Phys., 44 (1981) 593.

12. Sayers, D. E., Stern, E. A. and Lytle, F. W., Adv. X-ray Anal., 13 (1970) 248.

13. Lee, P. A., Citrin, P. H., Eisenberger, P. and Kincaid, B. M., Rev. Mod. Phys., 53 (1981) 769.

14. Stern, E. A. and Heald, S. M. in Koch. E. E. (ed.), Handbook on Synchrotron Radiation, Vol. 1, North-Holland, Amsterdam, 1983, Chapter 10, pp. 955-1014.

15. Hayes, T. M. and Boyce, J. B., Solid State Phys., 37 (1982) 173.

16. Teo, B. K. and Lee, P. A., J. Amer. Chem. Soc., 101 (1979) 2815.

17. Van Zon, J. B. A. D., Koningsberger, D. C., Van't Blick, H. F. J. and Sayers, D. E., J. Chem Phys., 82 (1985) 5742.

18. Teo, B. K., EXAFS Basic Principles and Data Analysis, Springer Verlag, Berlin (1986).

19. Dreier, P. and Rabe, P., Rev. Sci. Instrum., 57 (1986) 214.

20. Srivastava, U. C. and Nigam, H. L., Coordination Chemistry Reviews, 9 (1972) 275.

21. Kunzl, V., Trav. Cjim. Techecolovaquie, 4 (1932) 213.

22. Flank, A. M., Fontaine, A., Jucha, A., Lemonier, M., Raoux, D. and Williams, C., Nucl. Instr. Methods, Phys. Res., 208 (1983) 651.

23. Phizackerley, R. P., Rek, Z. V., Stephenson, G. B., Couradson, S. D., Hodgson, K. O., Matsushita, T. and Onyanayi, M., J. Appl. Cryst., 16 (1983) 220.

24. Eanes, E. D., Costa, J. L., MacKenzie, A. and Warburton, W. K., Rev. Sci. Instrum., 51 (1980) 1579.

25. Lu, K.-Q. and Stern, E. A., Nucl. Instrum. Methods Phys. Res., 212 (1983) 475.

26. Wong, J. Nucl. Instrum. Methods, Phys. Res., A238 (1985) 554.

27. McBreen, J., U.S. Patent 4,000,005, Dec. 28, 1976.

28. McBreen, J., O'Grady, W. E., Pandya, K. I., Hoffman, R. W. and Sayers, D. E., Langmuir, (1987) in press.

29. McMaster, W. H., Kerr Del Grande, N., Mallet, J. H. and Hubbell, J. H., Report UCRL - 50174, Lawrence Radiation Laboratory, University of California, Livermore.

30. CRC Handbook of Chemistry and Physics, Weast, R. C. and Astle, M. J., (eds.), CRC Press, Inc., Boca Raton, Florida (1981) pp. E-139-43.

31. O'Grady, W. E., Sayers, D. E., Budnick, J. I. and Hayes, G. H., Ext. Abst., No. 639, Electrochem. Soc. Proc. Vol. 85-1, 1985, p. 895-6.

32. Olender, H., McBreen, J., O'Grady, W. E., Srinivasan, S. and Kordesch, K. V., J. Electrochem. Soc., 129 (1982) 135.

33. Heald, S. M., in Koningsberger, D. C. and Prins, R., (eds.), Application Techniques of EXAFS, SEXAFS and XANES, John Wiley & Sons, New York (1987).

34. Wong, J., Mat. Sc. Eng., 80 (1986) 107.

35. Catlow, C. R. A. and Greaves, E. N., Chem. Br., 22 (1986) 805.

36. Robinson, A. L., Science, 235 (1987) 841.

37. Lagarde, P., Fontaine, A., Raoux, D., Sadoc, A. and Migliardo, P., J. Chem. Phys., 72 (1980) 3061.

38. Aliotte, F., Galli, G., Maisano, G., Migliardo, P., Vasi, C. and Wanderlingh, Nuovo Cimento, 2D (1983) 103.

39. McBreen, J., O'Grady, W. E., Sayers, D. and Yang, C. Y., Ext. Abst. No. 574, Electrochem. Soc, Proc. Vol. 86-1, 1986, p. 834-5.

40. Licheri, G., Pashcina, G., Piccaluga, G., Pinna, G. and Vlaic, G., Chem. Phys. Lett., 82 (1981) 384.

41. Beagley, B., Gahan, B., Greaves, G. N., McAuliffe, C. A. and White, E. W., J. Chem. Soc. Commun., 1804 (1985).

42. Sham, T. K., Hastings, J. B., Pearlman, M. L., Chem. Phys. Lett., 83 (1981) 391.

43. Pan, H. K., Yarusso, D. J., Knapp, G. S., Pineri, M., Meagher, A., Coey, J. M. D. and Cooper, S. L., J. Chem. Phys., 79 (1983) 4736.

44. Catlow, C. R. A., Chadwick, A. V., Greaves, G. N., Moroney, L. M. and Worboys, M. R., Solid State Ionics, 9 (1983) 1107.

45. Linford, R. G., Hall, P. G., Johnson, C. and Hasnian, S. S., Solid State Ionics, 14 (1984) 199.

46. Catlow, C. R. A., Chadwick, A. V., Greaves, G. N. and Moroney, L. M., J. Am. Ceram. Soc., 69 (1986) 272.

47. Moroney, L. M. and Sayers, D. E., J. Phys., 47 (1986) C8-725.

48. Battle, P. D., Catlow, C. R. A., Chadwick, A. V., Greaves, G. N. and Moroney, L. M., J. Phys., 47 (1986) C8-669.

49. Smith, D. A., Elder, R. C. and Heineman, W. R., Anal. Chem., 57 (1985) 2361.

50. McBreen, J., O'Grady, W. E. and Sayers, D., Ext. Abstr. No. 105, Electrochem. Soc. Proc. Vol. 86-2, 1986, p. 151-2.

51. Joyner, R. W. and Meehan, P., Vacuum, 33 (1983) 691.

52. Koningsberger, D. C., van Zon, J. B. A. D., van't Blik, H. F. J., Visser, G. J., Prins, R., Mansour, A. N., Sayers, D. E., Short, D. R. and Katzer, J. R., J. Phys. Chem., 89 (1985) 4075.

53. Koningsberger, D. C. and Sayers, D. E., Solid State Ionics, 16 (1985) 23.

54. Duivenoorden, F. B. M., Koningsberger, D. C., Uh, Y. S. and Gates, B. C., J. Am. Chem. Soc., 108 (1986) 6254.

55. Mansour, A. N., Sayers, D. E., Cook, Jr., J. W., Short, D. R., Shannon, R. D. and Katzer, J. R., J. Phys. Chem., 88 (1984) 1778.

56. O'Grady, W. E. and Koningsberger, D. C., J. Chem. Phys. (to be published).

57. Joyner, R. W., van Veen, J. A. R. and Sachtler, W. M. H., J. Chem. Soc., Faraday Trans. I, 78 (1982) 1021.

58. Cramer, S. P., Liang, K. S., Jacobsen, A. J., Chang, C. H. and Chianelli, R. R., Inorg. Chem., 23 (1984) 1215.

59. Hayes, T. M., Boyce, J. B. and Beeky, J. L., J. Phys., 11 (1978) 2931.

60. Sandstrom, D. R. and Lytle, F. W., Ann. Rev. Phys. Chem., 30 (1979) 215.

61. Lengeler, B., Z. Phys. B, 61 (1985) 421.

62. Sham, T. K., J. Chem. Phys., 79 (1983) 1116.

63. Linkous, C. A., O'Grady, W. E., Sayers, D. and Yang, C. Y., Inorg. Chem., 25 (1986) 3761.

64. Wong, J., Lytle, F. W., Messner, R. P. and Maylotte, D. H., Phys. Rev. B, 30 (1984) 5596.

65. Long, G. G., Druger, J. and Tanaka, D., J. Electrochem. Soc., 134 (1987) 264.

66. Gozzi, D., Tomellini, M., Bianconi, A. and Fanfoni, M., J. Electroanal. Chem., 198 (1986) 53.

67. Mansour, A. N., Cook, J. W. and Sayers, D. E., J. Phys. Chem., 88 (1984) 2330.

68. Gordon II, J. G., Melroy, O. R., Borges, G. L., Reisner, D. L., Abruna, H. D., Chandrasekhar, P. and Blum, L., J. Electroanal. Chem., 210 (1986) 311.

69. Kordesch, M. E. and Hoffman, R. W., Nucl. Instr. Methods Phys. Res., 222 (1984) 347.

70. Pandya, K. I., Yang, K., Hoffman, R. W., O'Grady, W. E. and Sayers, D. E., J. Phys., 47 (1986) C8-159.

71. Bedzyk, M. J., Bilderback, D., White, J., Abruna, H. D. and Bommarito, M. G., J. Phys. Chem., 90 (1986) 4926.

72. Stohr, J., Z. Phys. B, 61 (1985) 439.

73. Graeff, W., Z. Phys. B, 61 (1985) 469.

74. Yeager, E., Surf. Sci. 101 (1980) 1.

75. Raoux, D., Z. Phys. B, 61 (1985) 397.

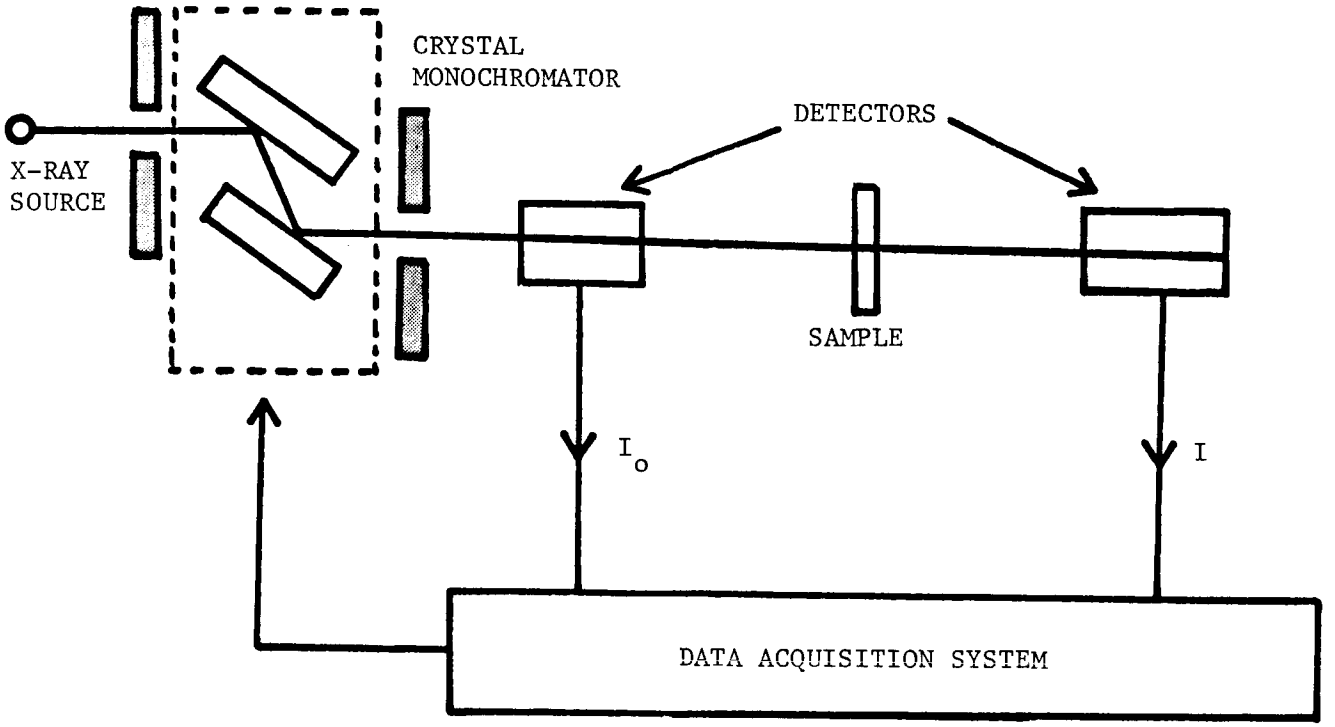

Figure 1. Experimental setup for transmission EXAFS measurements.

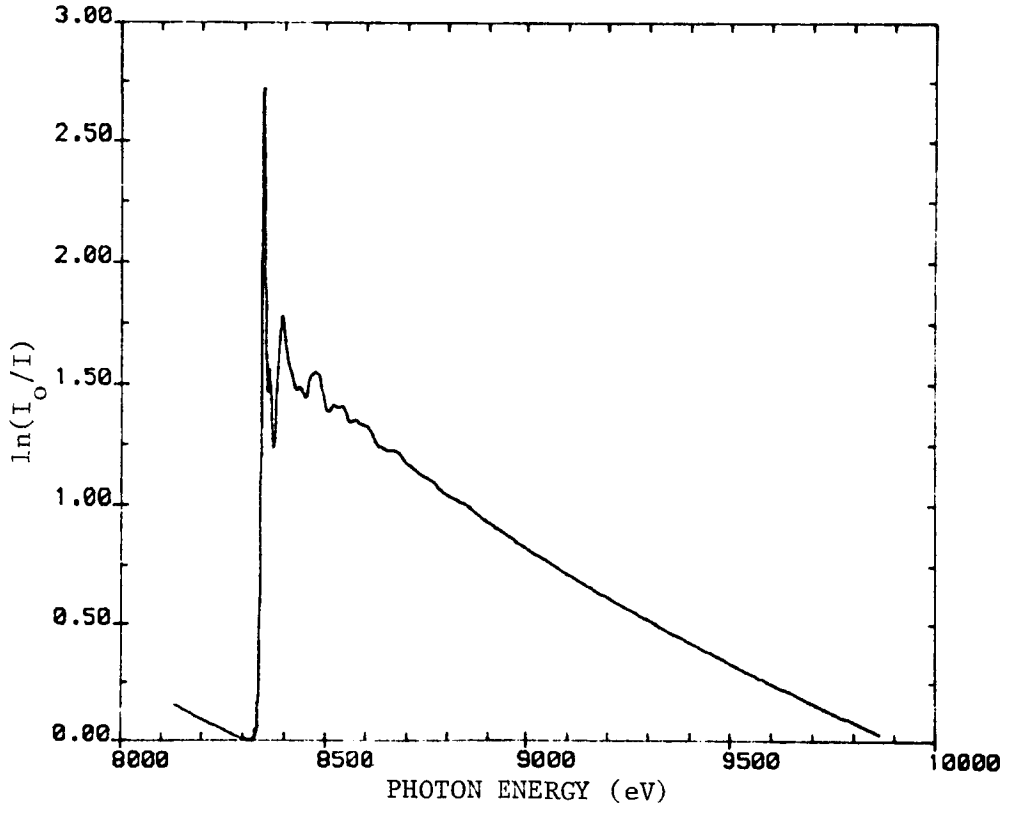

Figure 2. X-ray absorption spectrum for a plastic bonded nickel oxide electrode. The electrode composition was 52.6% $Ni(OH)_2$ + 4.2% $Co(OH)_2$ + 24.7% KS-2 graphite + 8.9% carbon fibers + 9.6% Kynar.

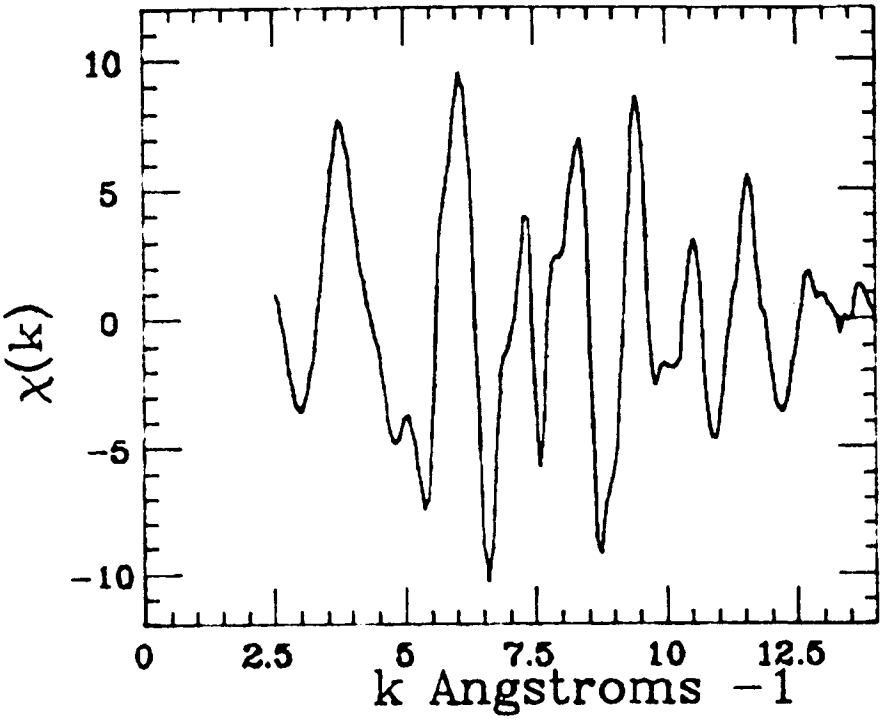

Figure 3. EXAFS from spectrum in Figure 2.

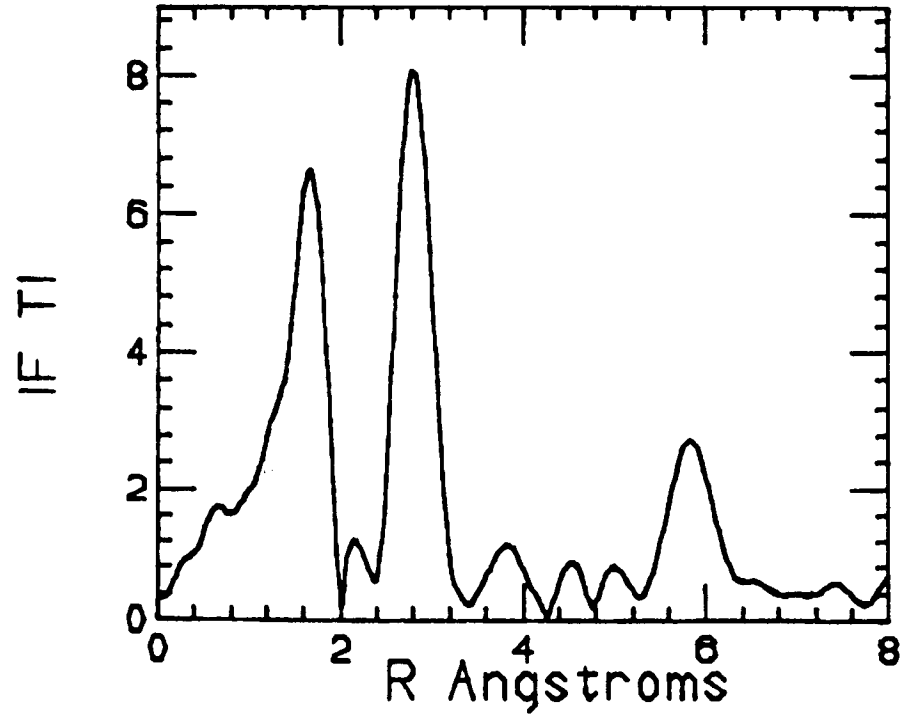

Figure 4. Fourier transform of data in Figure 3.

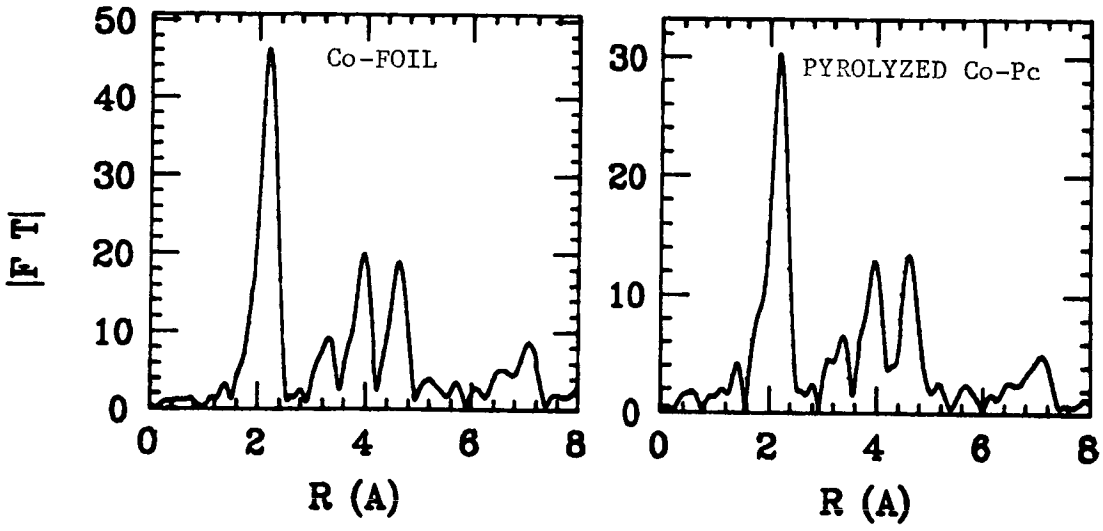

Figure 5. Radial structure functions for cobalt metal foil and cobalt phthalocyanine on Vulcan XC-72 carbon, after pyrolysis at 900°C.

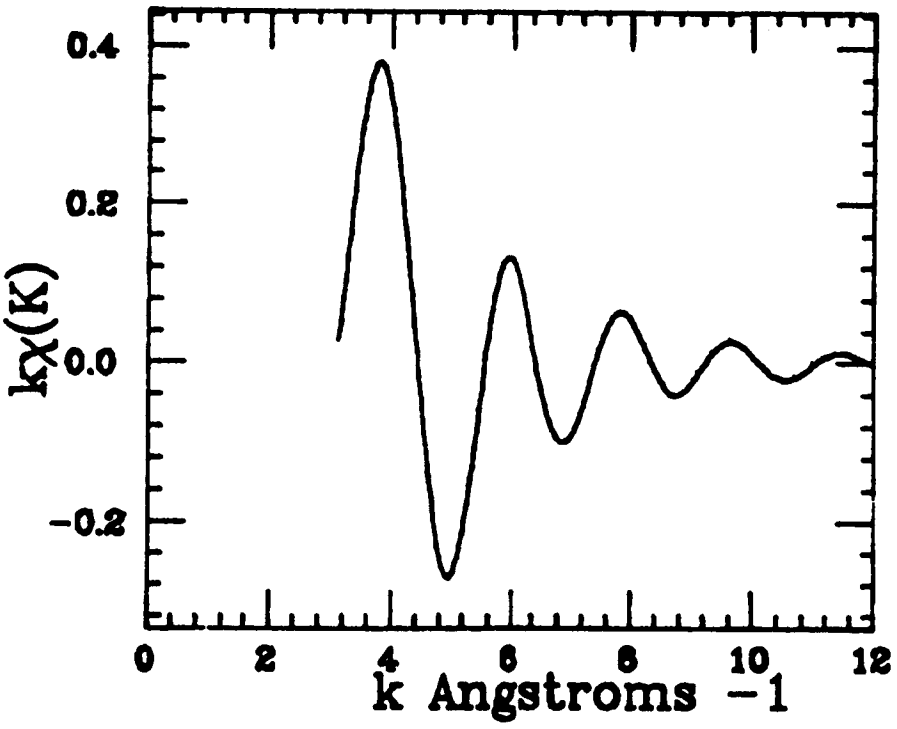

Figure 6. Inverse transform of the first peak of the Fourier transform in figure 4.

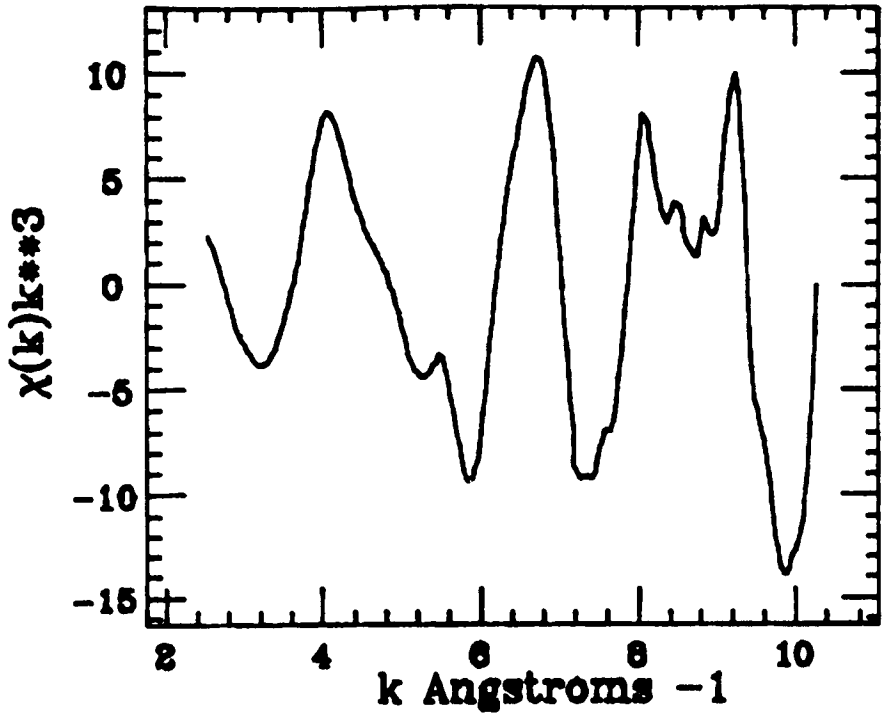

Figure 7. EXAFS for Co in electrode of figure 2.

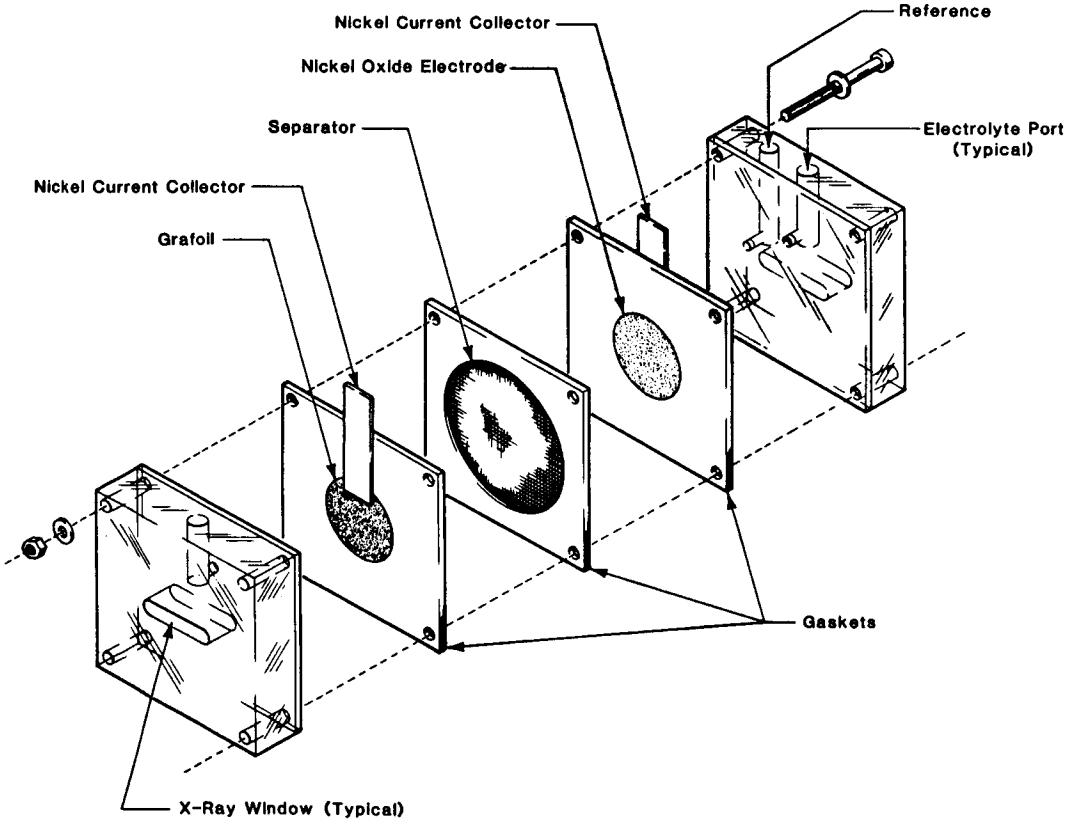

Figure 8. A cell for in situ studies of nickel oxide electrodes.

C-3

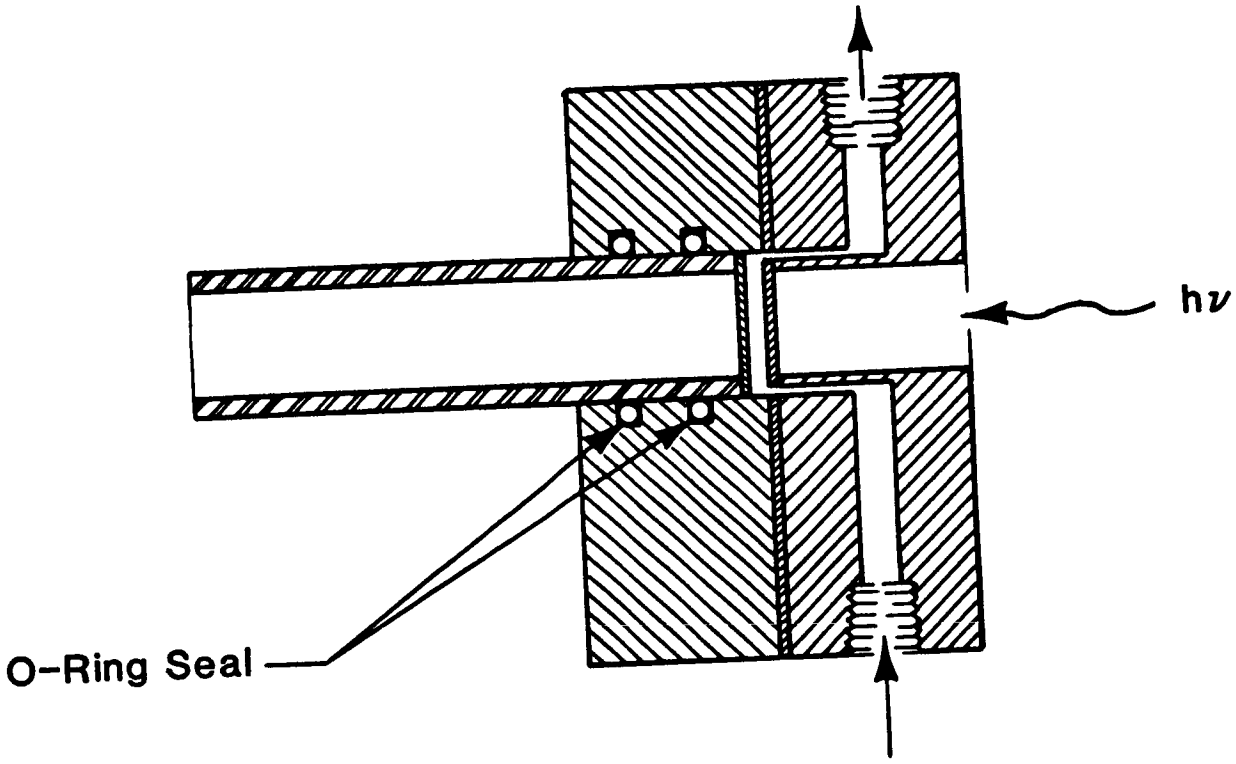

Figure 9. A cell for electrolyte EXAFS studies.